Science Advances
AAAS

advances.sciencemag.org/cgi/content/full/5/9/eaax1738/DC1

Supplementary Materials for

BAP1 regulates epigenetic switch from pluripotency to differentiation in developmental lineages giving rise to BAP1-mutant cancers

Jeffim N. Kuznetsov, Tristan H. Aguero, Dawn A. Owens, Stefan Kurtenbach, Matthew G. Field, Michael A. Durante, Daniel A. Rodriguez, Mary Lou King, J. William Harbour*

*Corresponding author. Email: harbour@miami.edu

Published 18 September 2019, *Sci. Adv.* **5**, eaax1738 (2019)
DOI: 10.1126/sciadv.aax1738

The PDF file includes:

Fig. S1. *X. laevis* and human Bap1 proteins show extensive sequence homology.
Fig. S2. Anatomic distribution of *Xenopus* bap1 mRNA and Bap1 protein expression during early development.
Fig. S3. Bap1 morpholinos and expression constructs.
Fig. S4. Developmental abnormalities in Bap1-deficient embryos are rescued by exogenous human BAP1.
Fig. S5. Loss of Asxl1 phenocopy loss of Bap1 during *Xenopus* development.
Fig. S6. Pharmacologic rescue of Bap1-deficient phenotype.
Fig. S7. Hdac4 is a key mediator of Bap1-deficient phonotype and acts independently of Hdac3 during development.
Fig. S8. Inhibition of HDAC4 significantly impairs proliferation of uveal melanoma cells in a BAP1-dependent manner.
Legends for data files S1 and S2

Other Supplementary Material for this manuscript includes the following:

(available at advances.sciencemag.org/cgi/content/full/5/9/eaax1738/DC1)

Data file S1 (Microsoft Excel format). Oligonucleotides and plasmids used in this study.
Data file S2 (Microsoft Excel format). Proteomic, transcriptomic, and epigenomic analyses.

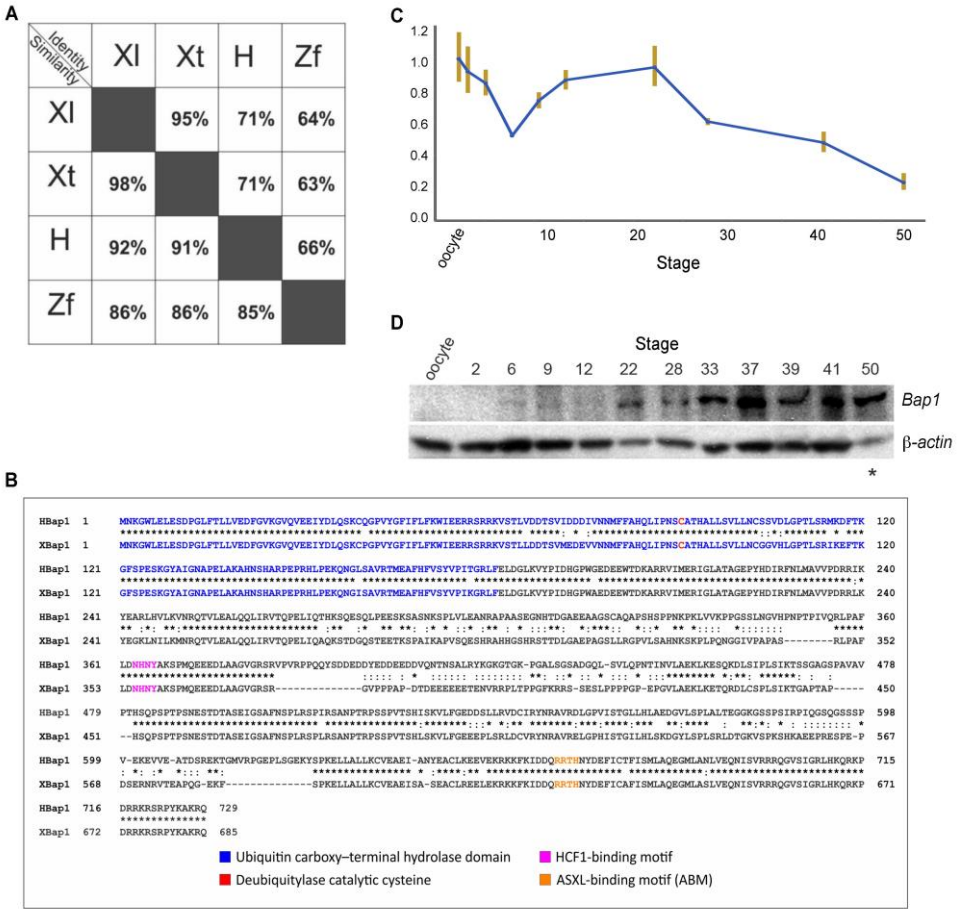

Fig. S1. *X. laevis* and human Bap1 proteins show extensive sequence homology. (**A**) Similarity and identity comparisons between *Xenopus laevis* (Xl), *Xenopus tropicalis* (Xt), human (H), and zebrafish (Zf) Bap1 proteins. (**B**) Sequence alignment of human and *Xenopus laevis* Bap1 proteins. (**C**) Expression of *bap1* mRNA by RT-qPCR at the indicated stages during *Xenopus laevis* early development (vertical yellow bars indicate standard error). (**D**) Detection of Bap1 protein by western blot at the indicated stages during *Xenopus laevis* early development. A total of 50 µg of protein was loaded into each lane, except for stage 50, in which 20 µg of protein lysate was used (*).

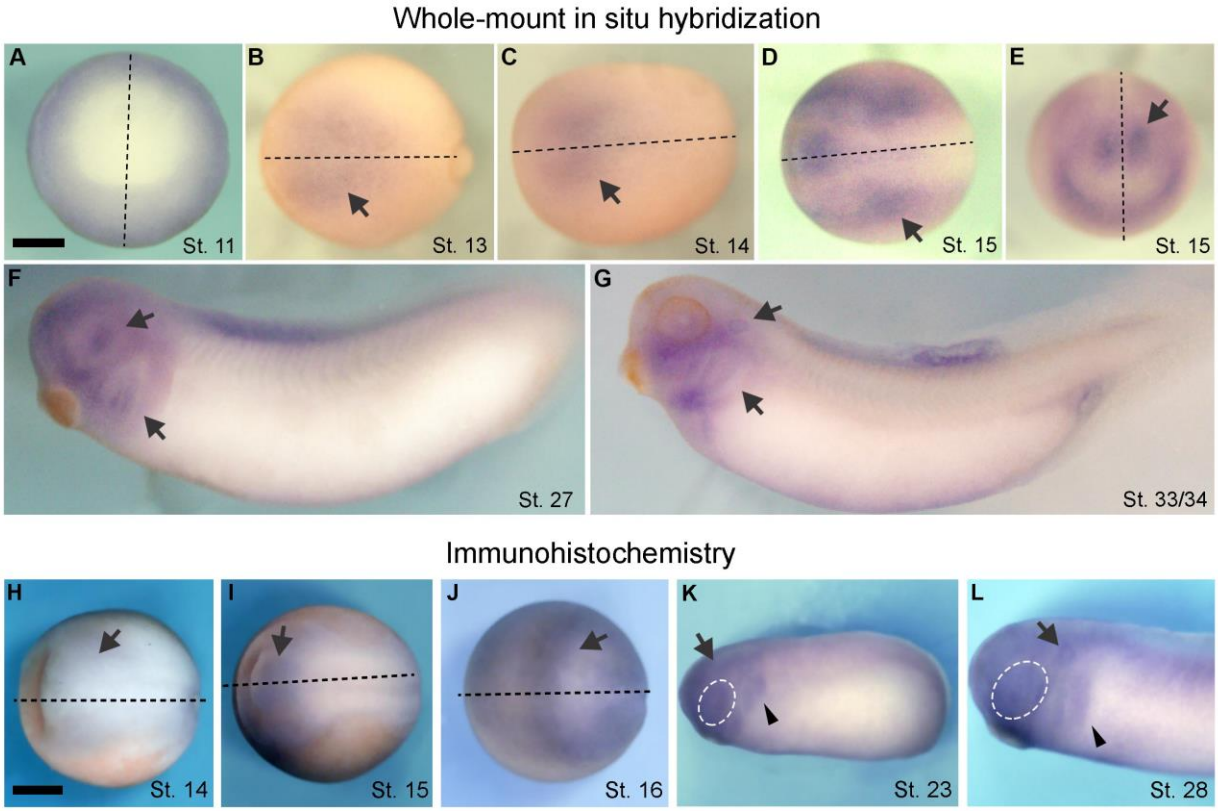

Fig. S2. Anatomic distribution of *Xenopus* bap1 mRNA and Bap1 protein expression during early development. (**A**) By whole-mount in situ hybridization, *bap1* mRNA (blue color) is located diffusely in early mesoderm and ectoderm at gastrulation. **(B-C**) *bap1* mRNA (arrows) becomes restricted to the early developing neural plate at stages 13-14. (**D-E**) Bap1 mRNA (arrows) is circumscribed at the lateral and anterior neural plate borders, including prospective neural crest, non-neural ectoderm, mid-brain, and sensorial placode, at stage 15. (**F**) During early tailbud stages, *bap1* mRNA is located in migrating cranial neural crest cells and optic vesicle (arrows). (**G**) In late tailbud stage, *bap1* mRNA is localized to branchial arches and otic vesicle (arrows). Panels show posterior view, dorsal at top (**A**), dorsal view, anterior side left (**B-D**), anterior at bottom, dorsal side up (**E**), and lateral view, anterior left (**F,G**). Dotted lines indicate midline; note symmetry of *bap1* expression. (**H-J**) By immunohistochemistry, Bap1 protein (arrows) is detected at the neural plate border during neurulation stages**.** (**K**) During early tailbud stages, Bap1 protein is localized to the eye field (dashed white oval), migrating cranial neural crest (arrowhead), and brain (arrow). (**L**) During later tailbud stages, Bap1 protein is mostly localized to eye field (dashed white oval), brachial arches (arrowhead), and otic vesicle (arrow). Panels show dorsal view, anterior side left (**A-C**), and lateral view, anterior side left (**K,L**). Dotted lines indicate midline. Scale bar: 250 μm.

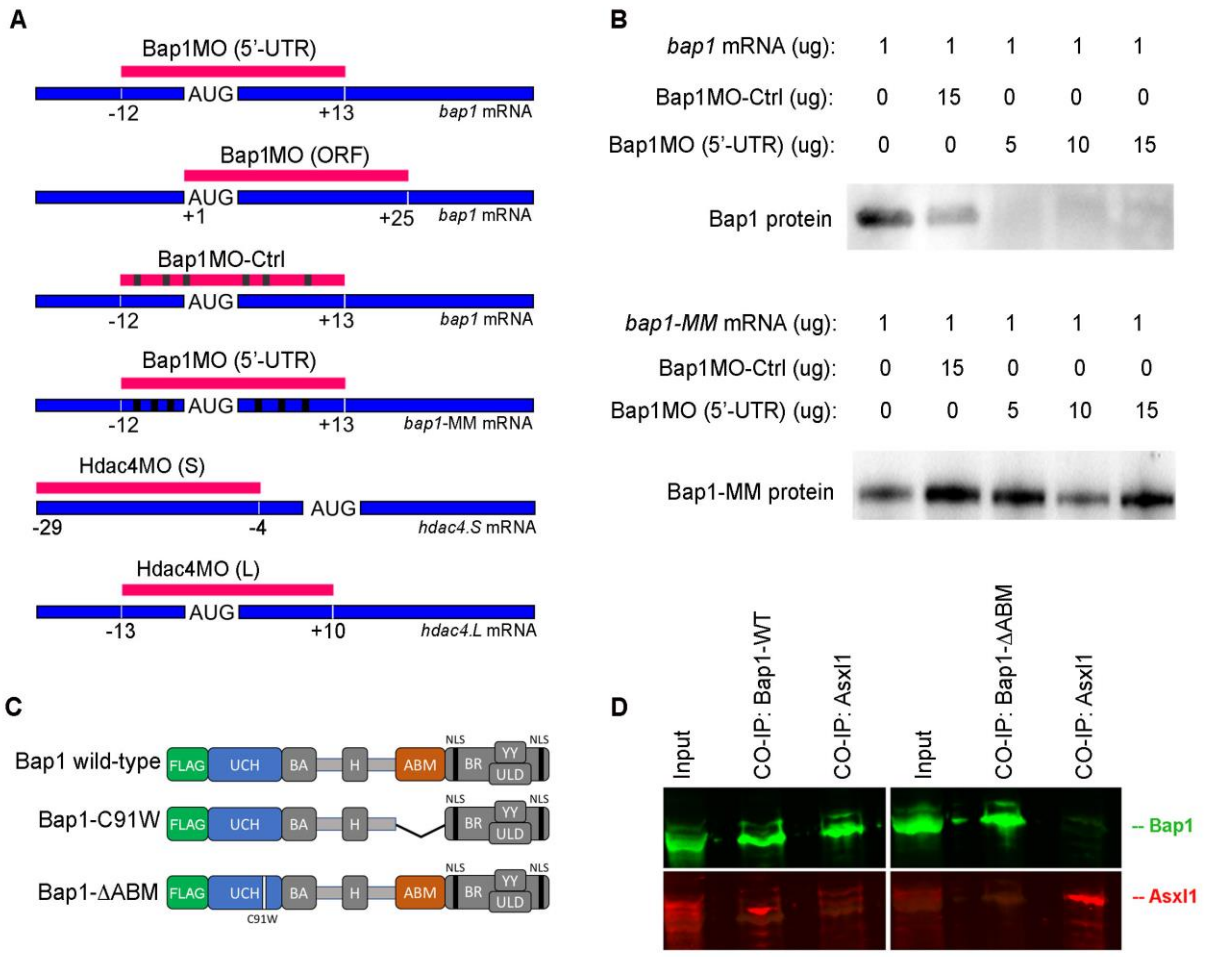

Fig. S3. Bap1 morpholinos and expression constructs. (**A**) Schematic representations of Bap1, Hdac3, Hdac4, and control morpholinos (red bars) and their binding sites within their targeted mRNAs (blue bars). Base-pair mismatches are indicated in black. (**B**) Validation of morpholino efficiency using *in vitro* wheat germ extracts for protein translation after incubating *bap1* mRNA with either control or increasing amounts of Bap1 morpholino (5'-UTR). (**C**) Schematic representations of recombinant proteins. Bap1ΔABM includes a deletion within the Asxl binding motif (ABM). Bap1-C91W contains a point mutation in the ubiquitin hydrolase catalytic cysteine. (**D**) Co-immunoprecipitation followed by western blot validating that the Bap1ΔABM mutant protein does not bind efficiently to Asxl1. Anti-FLAG (for Bap1) and Anti-V5 (for Asxl1) antibodies were used to detect Bap1 and Asxl1, respectively, as indicated.

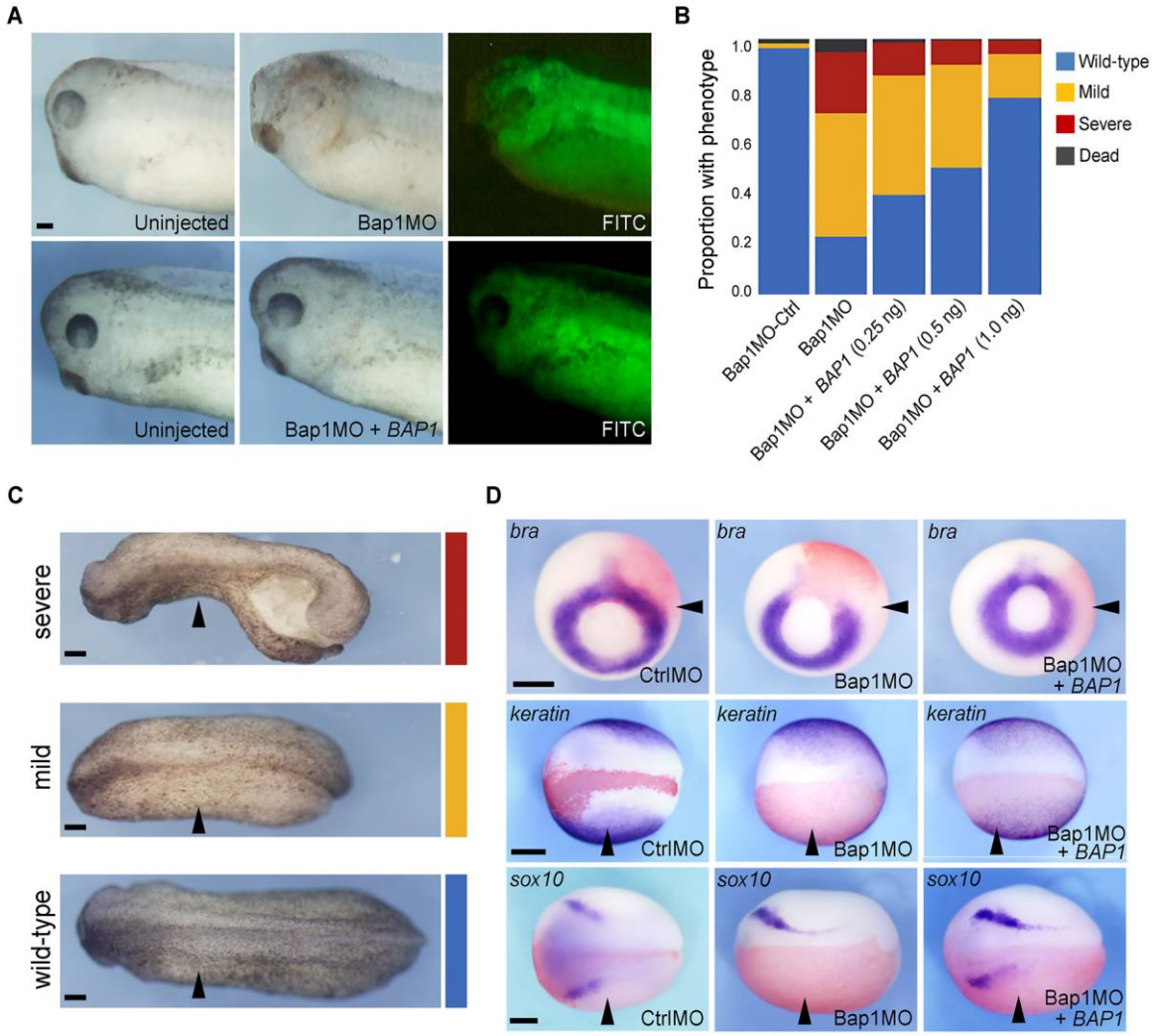

Fig. S4. Developmental abnormalities in Bap1-deficient embryos are rescued by exogenous human BAP1. (**A**) Representative embryos analyzed at late tailbud stage following injection into one blastomere at the two-cell stage of 7.5 ng Bap1MO or 7.5 ng Bap1MO plus 1 ng human *BAP1* mRNA, which is not recognized by Bap1MO. Fluorescein isothiocyanate (FITC) is a lineage tracer for the injected side (green). Microphthalmia eye defect is rescued by human BAP1 mRNA. Panels show lateral view, anterior left. (**B**) Human *BAP1* mRNA rescues the failure of embryo development, associated with Bap1 loss, in a dose-dependent manner. Embryos were injected with 7.5 ng Bap1MO plus human *BAP1* mRNA and analyzed at early tailbud stages (n=300 embryos from three different females, >90% with phenotype) (**C**) Visual representation of embryos summarized in B, showing the human *BAP1* mRNA rescue effect ranging from indistinguishable from wild-type (blue), to mild mesodermal foreshortening (yellow) to severe spina bifida (red). Panels show dorsal view, anterior left. **(D)** Representative embryos at gastrula and neurula stages treated as above and analyzed by whole mount *in situ* hybridization, demonstrating that failed expression of the indicated developmental genes in Bap1-deficient embryos was rescued by human *BAP1* mRNA. Panels show posterior view, dorsal side up (top row), and dorsal view, anterior left (middle and bottom rows). Scale bar: 250 μm.

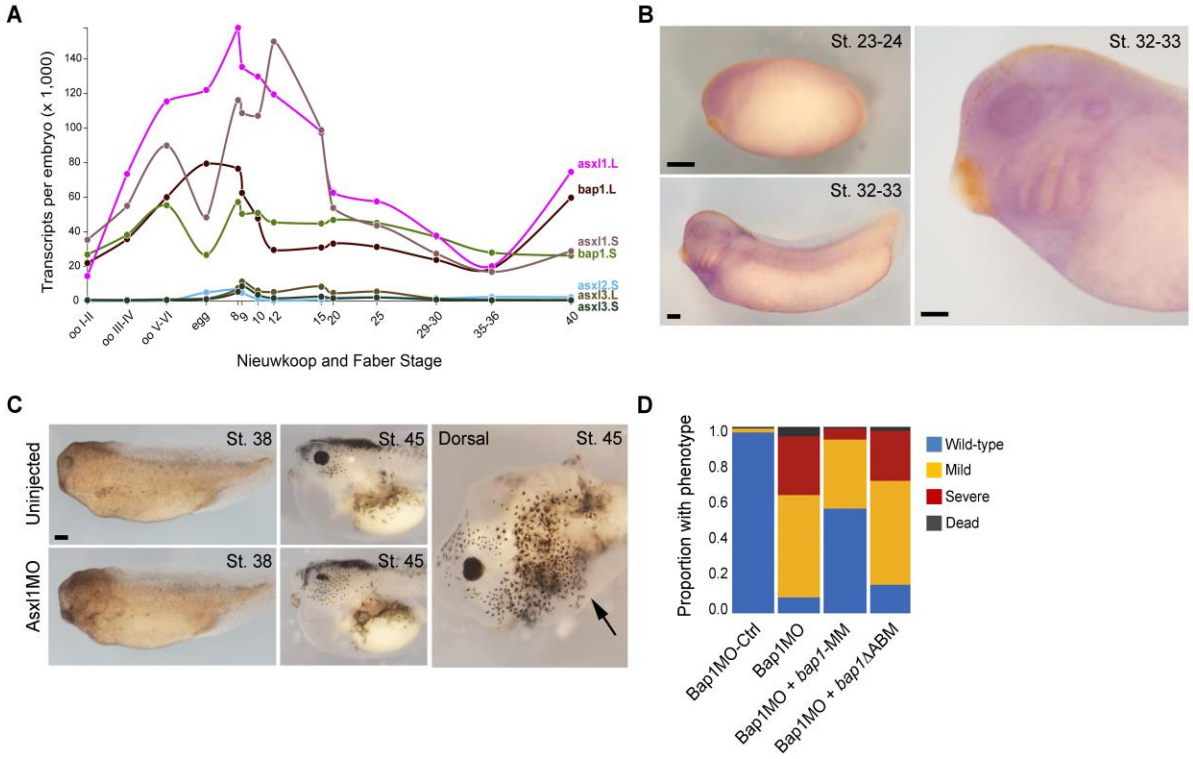

Fig. S5. Loss of Asxl1 phenocopy loss of Bap1 during *Xenopus* development. (**A**) RNA-seq global expression profiling of *bap1*, *asxl1*, *asxl2* and *asxl3* during *Xenopus* development (Xenbase.org), showing strongest correlation between *bap1* and *asxl1* expression. L and S indicate transcripts from long and short chromosomes, respectively. (**B**) Anatomic distribution of *asxl1* mRNA expression at the indicated stages of *Xenopus laevis* development analyzed by whole mount *in situ* hybridization, showing strong similarity to *bap1* expression pattern. Panels show lateral view, anterior left. (**C**) Representative embryos analyzed at the indicated stages following injection into one blastomere at the two-cell stage of 10 ng of Asxl1MO. Asxl1-deficiency phenocopied axial foreshortening, microphthalmia and abnormal melanocyte phenotype observed with Bap1-deficiency (see Fig. 1). Panels show lateral view, anterior left, except right panel showing dorsal view, anterior side down (arrow indicates injected side). (**D**) Summary of rescue experiments using either morpholino-resistant *Xenopus bap1* (*bap1*-MM) or *bap1* containing a mutation at the Asxl binding motif (*bap1*ΔABM) to rescue the Bap1-deficient phenotype caused by Bap1MO (n=300 embryos from three different females, >85% with phenotype, analyzed at late tailbud stages). In contrast to *bap1*-MM, co-injection with *bap1*ΔABM provided no rescue, indicating that Bap1 requires interaction with Asxls for its developmental functions. Scale bar: 250 μm.

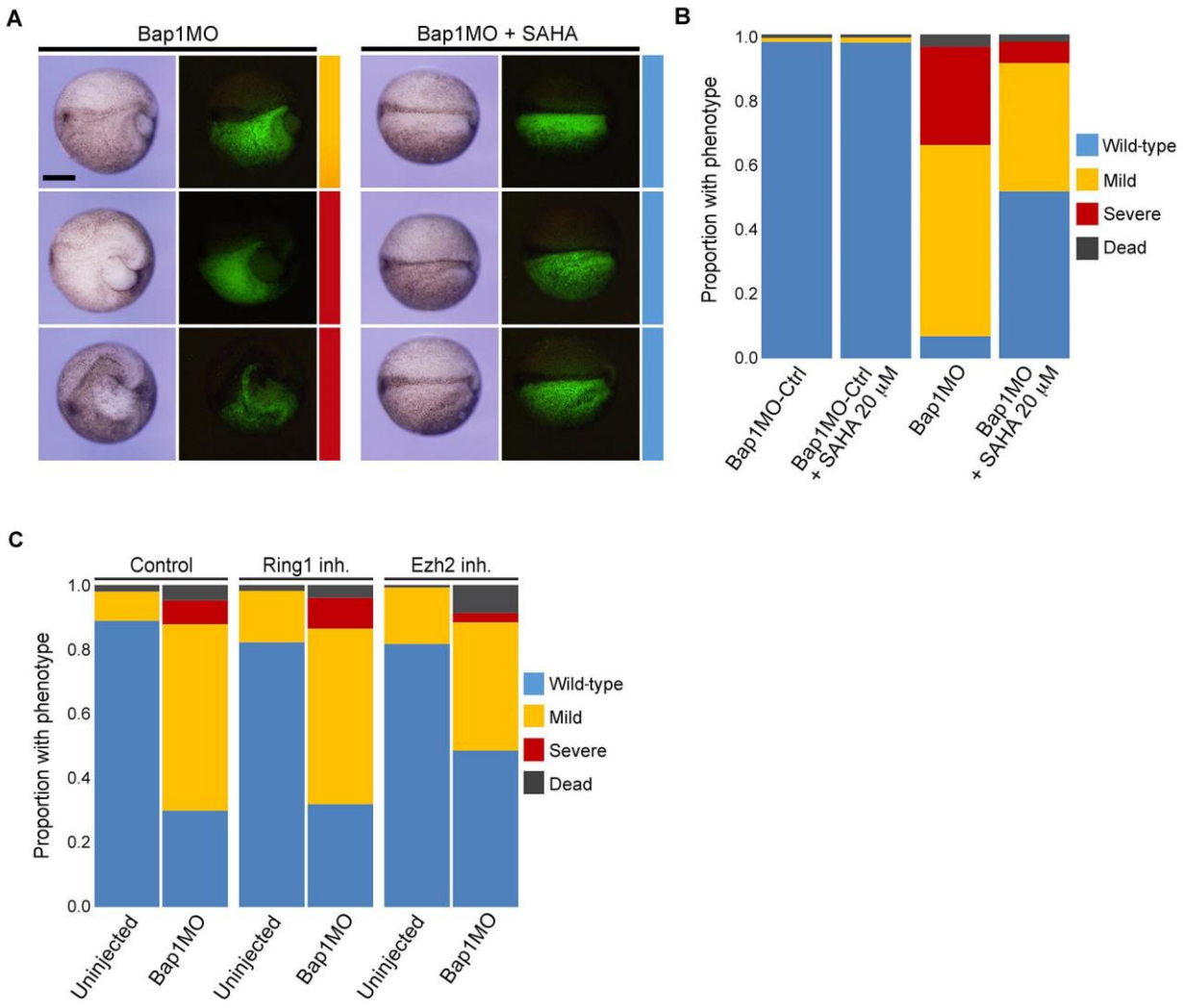

Fig. S6. Pharmacologic rescue of Bap1-deficient phenotype. (**A**) Treatment of embryos with pan-histone deacetylase inhibitor SAHA at mid-neurula (stage 14-16) following injection into one blastomere at two-cell embryo stages with 7.5 ng Bap1MO and incubated from blastula to neurula stages (stage 9 to 15) with DMSO alone (left 2 columns) or with 20 µM SAHA in DMSO (right 2 columns). Fluorescence images are shown to the right of each corresponding color image to demonstrate FITC as a tracer for the injected side (green). (**B)** Summary of experiments (n=300 embryos from three different females, >90% with phenotype), showing substantial rescue of Bap1-deficient phenotype with SAHA treatment and lack of toxicity in control Bap1MO-Ctrl injected embryos. (**C)** Summary of results (n=835 embryos from three different females, >90% with phenotype) using the Ring1 inhibitor (PRC1 complex) PRP4165 and the Ezh2 inhibitor (PRC2 complex) GSK126, neither of which demonstrated rescue of the Bap1-deficient phenotype. Embryos were analyzed at mid-neurula (stage 14-16) following injection into one blastomere of two-cell embryos with 7.5 ng Bap1MO and incubated either with 20 µM PRT4164 or 25 µM GSK126 from blastula to early neurula stages (stage 9 to 13). Scale bar: 250 µm.

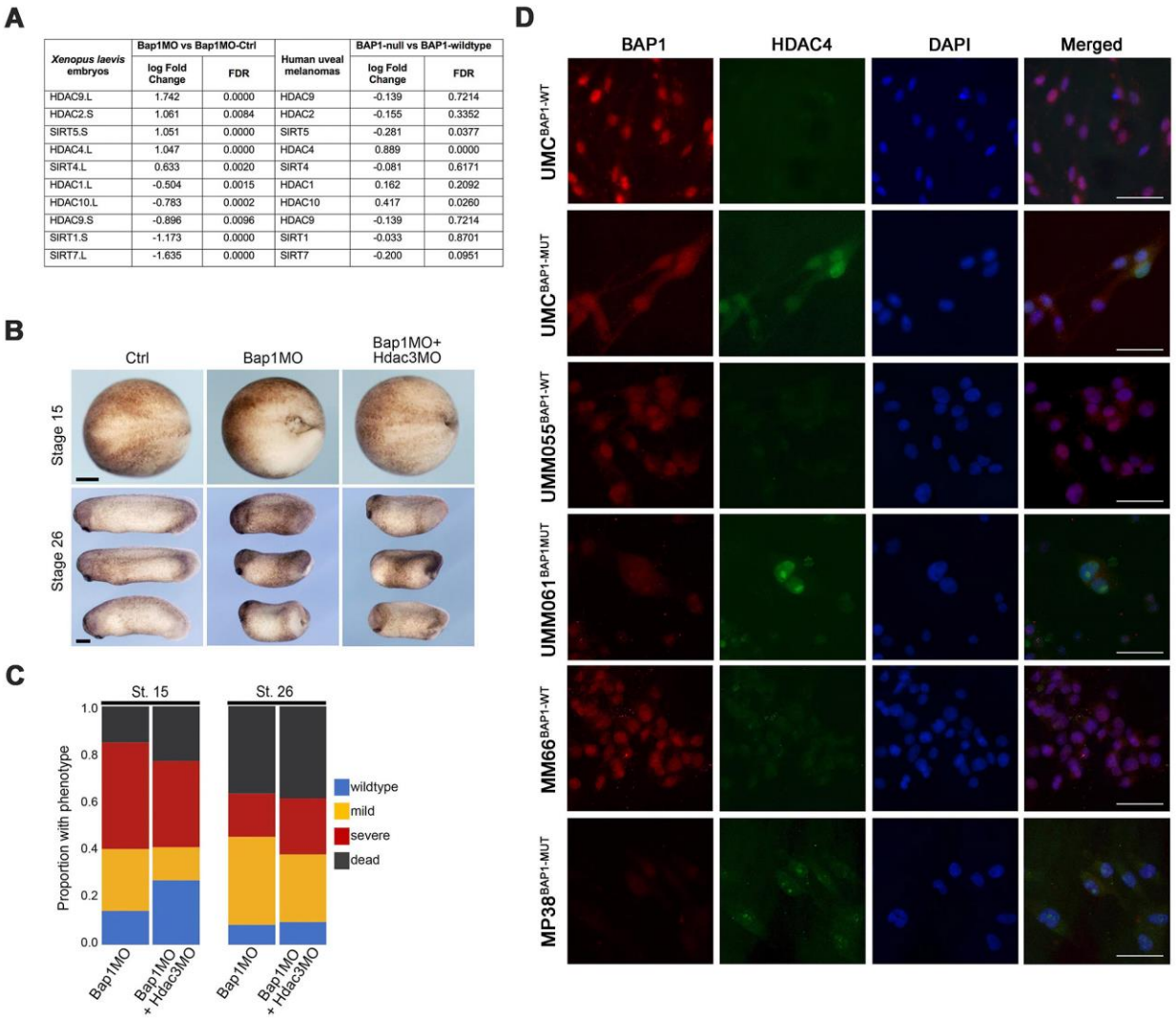

Xenopus laevis embryos	Bap1MO vs Bap1MO-Ctrl		Human uveal melanomas	BAP1-null vs BAP1-wildtype	
	log Fold Change	FDR		log Fold Change	FDR
HDAC9.L	1.742	0.0000	HDAC9	-0.139	0.7214
HDAC2.S	1.061	0.0084	HDAC2	-0.155	0.3352
SIRT5.S	1.051	0.0000	SIRT5	-0.281	0.0377
HDAC4.L	1.047	0.0000	HDAC4	0.889	0.0000
SIRT4.L	0.633	0.0020	SIRT4	-0.081	0.6171
HDAC1.L	-0.504	0.0015	HDAC1	0.162	0.2092
HDAC10.L	-0.783	0.0002	HDAC10	0.417	0.0260
HDAC9.S	-0.896	0.0096	HDAC9	-0.139	0.7214
SIRT1.S	-1.173	0.0000	SIRT1	-0.033	0.8701
SIRT7.L	-1.635	0.0000	SIRT7	-0.200	0.0951

Fig. S7. Hdac4 is a key mediator of Bap1-deficient phonotype and acts independently of Hdac3 during development. (**A**) Comparison of RNA-seq data from *Xenopus laevis* embryos and 80 human uveal melanoma samples from TCGA to identify histone deacetylases that are differentially expressed in association with BAP1 loss. (**B**) Representative embryos injected at the 1-cell stage with 15 ng of Bap1MO with or without 8 ng of a morpholino directed against Hdac3 (Hdac3MO), analyzed at mid-neurula stage (stage 15, dorsal view, anterior to left) and early tailbud stage (stage 26, lateral view, anterior to left). Scale bar: 250 μm. (**C**) Quantification of results depicted in B, showing no rescue of the Bap1-deficient phenotype by Hdac3MO (n=200 embryos from 2 females, >90% with phenotype). (**D**) Immunofluorescence imaging using antibodies against HDAC4 and BAP1 on normal human uveal melanocytes (UMC) that are wild-type for BAP1 (WT) or engineered to express a truncated inactive BAP1 protein using CRISPR/Cas9 (MUT). Primary uveal melanoma cells with wild-type BAP1 (UMM055 and MM66) or mutationally inactivated for BAP1 (UMM061 and MP38) were also examined. Scale bar: 50 μm.

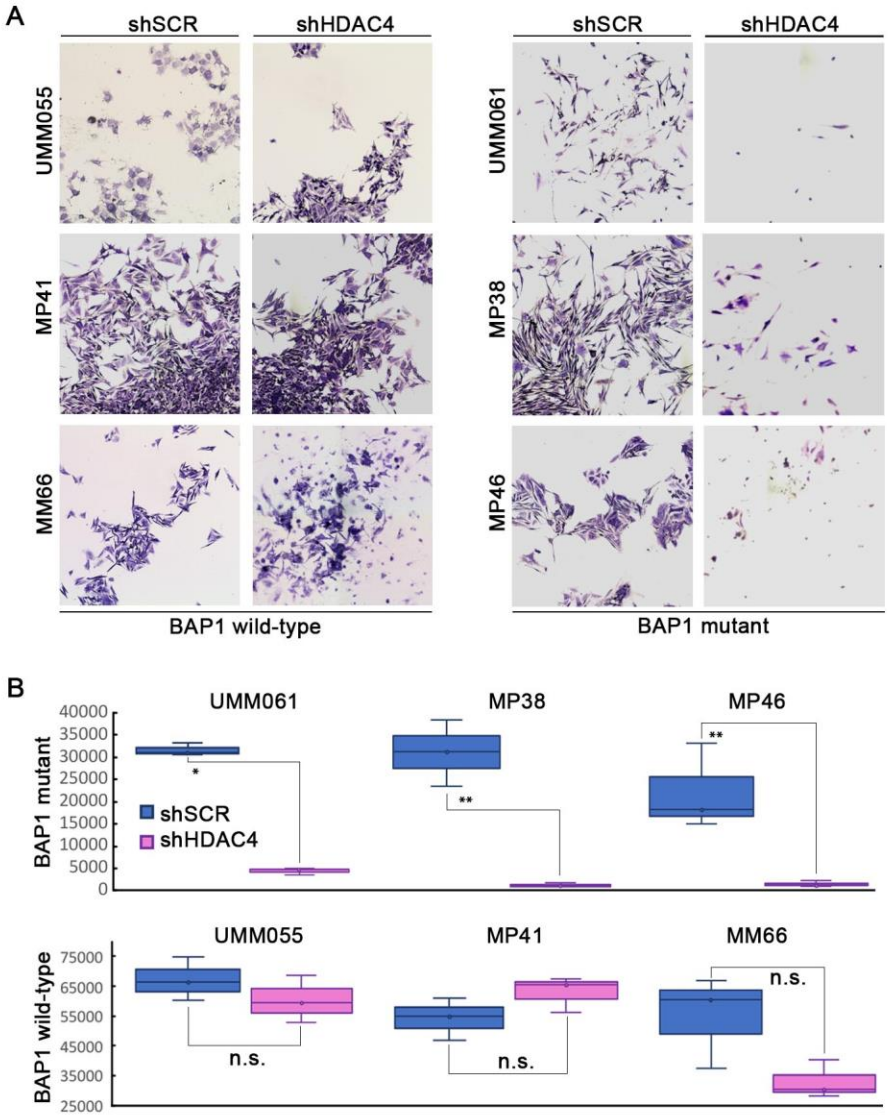

Fig. S8. Inhibition of HDAC4 significantly impairs proliferation of uveal melanoma cells in a BAP1-dependent manner. (**A**) Uveal melanoma cell lines with wild-type BAP1 (UMM055, MP41, and MM66) or with mutant BAP1 (UMM061, MP38, and MP46) were engineered to express shHDAC4 or control scrambled shSCR and plated at equal numbers ($2x10^3$/well) and cultured for 2 weeks, after which they were stained with crystal violet and imaged under 20X magnification. BAP1-wildtype cells and control BAP1-mutant cells demonstrated typical morphology and growth, whereas BAP1-mutant cells expressing shHDAC4 demonstrated senescence phenotype and increased cell death. (**B**) To quantitate these findings, viable cells were counted using ImageJ. Each experiment was performed in triplicate. *P* values were determined by two-tailed t-test. **P*<0.001, ***P*<0.05; n.s., not significant.

Supplemental Data Legends

Data file S1. Oligonucleotides and plasmids used in this study.

Data file S2. Proteomic, transcriptomic, and epigenomic analyses. (**A**) Mass spectrometry of Bap1 interacting proteins in *Xenopus laevis* stage 12 embryos. (**B**) RNA-seq data from *Xenopus laevis* stage 12 embryos analyzed for differentially expressed genes in wild-type and Bap1-knockdown embryos. (**C**) Quantification of ChIP-seq signals for H3K27ac, H3K27me3, H3K4me3 and H2AK119ub around transcription start sites ± 2 kb. (**D**) Subset of genes with decrease in H3K27ac signal >40% and corresponding decrease in RNA-seq gene expression logFC < -0.6 in Bap1-knockdown stage 12 embryos compared to embryos injected with CtrlMO.